Available online at www.sciencedirect.com
ScienceDirect
Geochimica et Cosmochimica Acta 71 (2007) 1232–1248
Geochimica
www.elsevier.com/locate/gca

Sources of mud volcano fluids in the Gulf of Cadiz—indications for hydrothermal imprint

Christian Hensen [a,*], Marianne Nuzzo [b], Edward Hornibrook [b], Luis M. Pinheiro [c,d], Barbara Bock [a], Vitor H. Magalhães [c,d], Warner Brückmann [a]

[a] Leibniz-Institute of Marine Sciences, IFM-GEOMAR, Wischhofstr. 1–3, D-24148 Kiel, Germany
[b] Bristol Biogeochemistry Research Centre, Department of Earth Sciences, University of Bristol, UK
[c] CESAM and Geosciences Department, Universidade de Aveiro, Aveiro, Portugal
[d] Marine Geology Department, INETI, Alfragide, Portugal

Received 16 February 2006; accepted in revised form 20 November 2006

Abstract

Mud volcanism in the Gulf of Cadiz occurs over a large area extending from the shelf to more than 3500 m water depth and is triggered by compressional stress along the European–African plate boundary, affecting a deeply faulted sedimentary sequence of locally more than 5 km thickness. The investigation of six active sites shows that mud volcano (MV) fluids, on average, are highly enriched in CH_4, Li, B, and Sr and depleted in Mg, K, and Br. The purity of the fluids is largely controlled by the intensity of upward directed flow. Flow rates could be constrained by numerical modelling and vary between <0.05 and 15 cm yr^{-1}. Application of δD–$\delta^{18}O$ systematics identifies clay mineral dehydration, most likely within Mesozoic and Tertiary shales and marls, as the major source of fluids. Hence, Cl and Na in the pore fluids are mostly depleted below seawater values, following a general trend of dilution. However, deviations from this trend occur and are likely caused by the dissolution of halite in evaporitic deposits. Other secondary processes overprinting the original fluid composition may occur along the flow path, such as dissolution of anhydrite or gypsum and/or the formation of calcite and dolomite. Different sources of fluids are also indicated by variations in $^{87}Sr/^{86}Sr$, which range from 0.7086 to 0.7099 at the different sites. Dehydration may be induced primarily by overburden and tectonic compression; however, very high concentrations of Li and B, specifically at Captain Arutyunov MV (CAMV) indicate additional leaching at temperatures above 150 °C, which could be explained by the injection of hot fluids along deep penetrating, major E–W strike–slip fault systems. This hypothesis is supported by the occurrence of generally thermogenic, but significantly CH_4-enriched, light volatile hydrocarbon gases at CAMV which cannot be explained by shallow microbial methanogenesis. Li and Li/B ratios from different types of hot and cold vents are used to infer that high temperature signals seem to be preserved at various cold vent locations and indicate a closer coupling of both systems in continental margin environments than outlined in previous studies.

1. Introduction

Mud volcanism provides an important, but poorly constrained transport pathway for fluids along continental margins. Several thousands of mud volcanoes (MVs) may occur in deep-water areas along continental margins (Milkov, 2000; Milkov et al., 2003) so that the expulsion of sedimentary fluids at continental margins may play a significant role for global fluid and element budgets (Aloisi et al., 2004a). Fluid expulsion is generally coupled to tectonic activity controlling episodic fault displacements (Moore and Vrolijk, 1992). Mud volcanoes and other types of cold vent systems are offering a window into otherwise obscured deep structural and diagenetic processes as geochemical interactions of the rising fluid with surrounding sediment and rock may significantly alter the chemistry of the pore fluids. Such diagenetic processes may involve

* Corresponding author. Fax: +49 431 6002928.
E-mail address: chensen@ifm-geomar.de (C. Hensen).

0016-7037/$ - see front matter © 2006 Elsevier Inc. All rights reserved.
doi:10.1016/j.gca.2006.11.022

the degradation of organic matter and the formation of gas hydrates (e.g. Martin et al., 1993; Buffett and Archer, 2004; Hensen and Wallmann, 2005), mineral dissolution/precipitation reactions and transformation processes of clay minerals and volcanic ashes (Chan and Kastner, 2000; Brown et al., 2001; Dählmann and De Lange, 2003) and high-temperature reactions with oceanic or continental crust (Martin et al., 1991; You and Gieskes, 2001; Von Damm et al., 2005). Negative chloride anomalies are typically reported from many modern accretionary prisms (Moore and Vrolijk, 1992); however, depending on the geologic and structural setting, the overlap of a number of these processes may lead to the formation of geochemically distinct fluids with an eventually complex history. This problem has been addressed by a number of studies (e.g. Martin et al., 1996; Suess et al., 1998; Fryer et al., 1999; Haese et al., 2003; Aloisi et al., 2004a; Hensen et al., 2004) which have helped to improve our knowledge of key processes involved. Moreover, any rising fluid may be subject a large number of processes occurring simultaneously or successively under regionally changing environmental conditions. Hence, in many cases there is no unambiguous solution for the origin of a specific fluid. In some cases ODP drilling data provided valuable information bridging the gap between subsurface processes and sea floor observations. In order to proceed towards a more general understanding of deep structural control on cold venting more systematic investigations from various tectonic settings are required.

Although the Gulf of Cadiz is, at present, target area of a number of European projects, geochemical data published to date are mostly limited to thermogenic hydrocarbon gases and CH_4 clathrates from MVs situated on the Moroccan Margin (Mazurenko et al., 2003; Depreiter et al., 2005; Van Rensbergen et al., 2005; Stadnitskaia et al., 2006). Here, we provide the first comprehensive data set on the geochemistry of mud volcano fluids in the Gulf of Cadiz. We combine analysis of pore water and gas geochemistry with information on regional geology to unravel the origin of the fluids in this compressive margin, which may be undergoing active subduction, as suggested recently by (Gutscher et al., 2002).

2. Study area and geological background

The Gulf of Cadiz is located in a structurally complex convergent tectonic setting in which the boundary between the African and Eurasian plates is concealed beneath thick (~7 km) Mio-Pliocene sedimentary deposits (e.g. Medialdea et al., 2004). In this area the Africa–Eurasia plate boundary strikes from the right-lateral Gloria Fault and Bank of Gorringe thrust to the west, to the Alboran Sea, east of the Strait of Gibraltar (Fig. 1). The region is seismically active (Buforn et al., 1995; Ribeiro et al., 1996) and

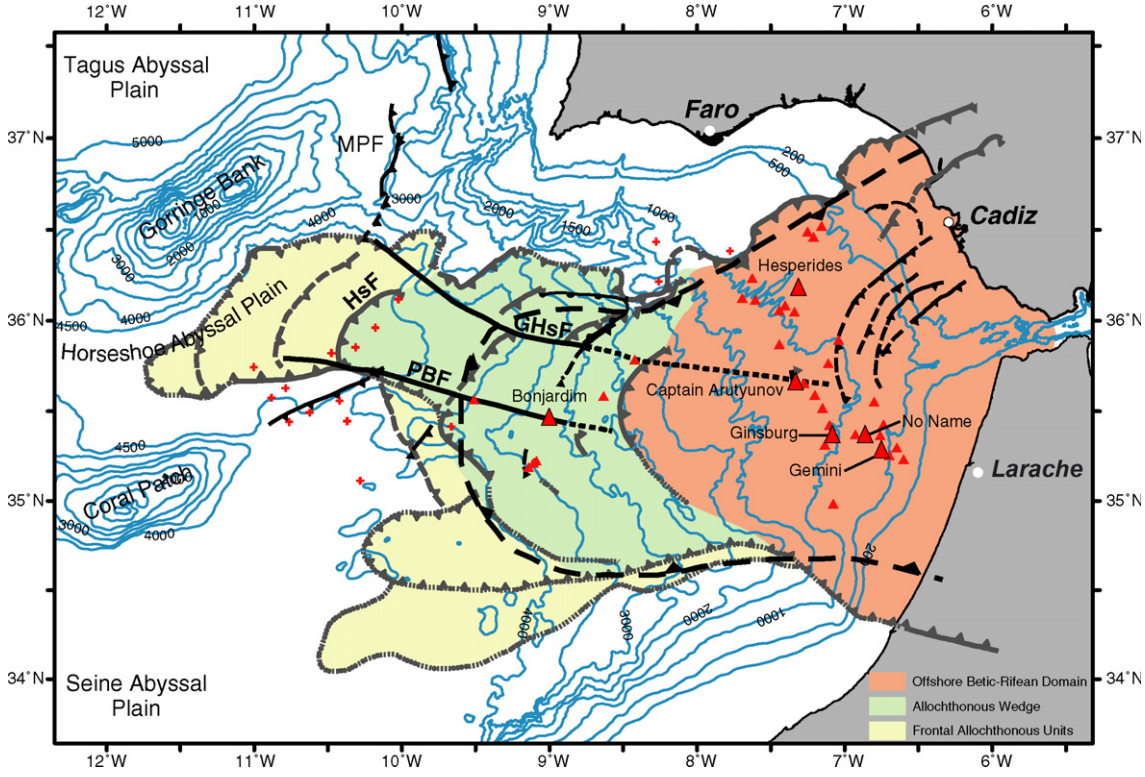

Fig. 1. Simplified structural geology map of the Gulf of Cadiz, modified after (Medialdea et al., 2004) and complemented with interpretations based on the Matespro bathymetric survey (Duarte et al., 2005), showing the Betic–Rifain Domain, the Allochthonous Wedge, the Frontal Allochtonous Units, major faults (black), the locations of Captain Arutyunov, Bonjardim, Ginsburg, Gemini, Hesperides, and No Name MVs (large triangles), and other MVs (small triangles) in the region. Major tectonic features include the Marques de Pombal (MPF), Porto-Bonjardim (PBF), Horseshoe (HsF), and Gorringe-Horseshoe (GHsF) Fault. Crosses are basement highs. The large thrust fault outline (dashed line) indicates the edge of the accretionary wedge as suggested by Gutscher (2004). Bathymetric contours are from the GEBCO 2003 database.

was the epicentre of an >8.5 magnitude earthquake in 1755 which, combined with an associated tsunami, decimated the city of Lisbon, Portugal (Baptista et al., 1988). The NE sector is marked by a conjugate set of NW–SE and NE–SW strike–slip faults (Fig. 1) that control diapiric ridges and together with major WNW–ESE strike–slip faults are thought to accommodate the NW-directed plate convergence (e.g. Argus et al., 1989; Pinheiro et al., 2005) in a broad deformation zone (Morel and Meghraoui, 1996) that has been described as a diffuse plate boundary (Sartori et al., 1994). It has been proposed previously that plate convergence in the region is accommodated along major deeply rooted Paleozoic wrench faults reactivated under Plio-Quaternary transpressive convergence (Meghraoui et al., 1996; Morel and Meghraoui, 1996). The formation of the Arc of Gibraltar and expulsion of thick nappes to the west in the Gulf of Cadiz were initiated by a change in the main convergence direction during the Mid- to Upper-Miocene (Maldonado et al., 1999). Several studies have suggested that westward progression of the Arc of Gibraltar into the Gulf of Cadiz ceased before the Pliocene (e.g. Lonergan and White, 1997; Maldonado et al., 1999), however, Gutscher et al. (2002) and Gutscher (2004) proposed that E–W subduction remains active and is driven by the rollback of a relic of subducted Thethian oceanic crust beneath the Arc of Gibraltar (Fig. 1).

Mud volcanoes (MVs) were first discovered and sampled in the Gulf of Cadiz in 1999 (Gardner, 2001) and since then have been extensively investigated during several research cruises (Pinheiro et al., 2003, 2005). Folding, mud volcanism, and diapirism in the region result from neo-tectonism (Gràcia et al., 2003) and MVs are located either along major strike–slip faults or at the intersection of these faults with arcuate thrusts associated with the formation of the Gibraltar Arc (Pinheiro et al., 2003, 2005).

3. Material and methods

In December 2003, an extensive scientific programme was conducted on the German research vessel *RV Sonne* (cruise SO 175-2; Kopf and participants, 2004). Sediments, fluids, and gases were sampled from active MVs throughout the Gulf (Fig. 1 and Table 1). Surface indications for active seepage of methane-rich fluids were not observed at any of the sites during this cruise, i.e. there was an absence of typical chemosynthetic fauna (Kopf and participants, 2004), but widespread evidence for anaerobic oxidation of methane (AOM) occurring in the shallow subsurface (Niemann et al., 2006). The sites sampled were Captain Arutyunov MV (CAMV, GeoB 9036-2, 9041-1, 9072-1), Ginsburg MV (GeoB 9061-1), Bonjardim MV (GeoB 9051-1, 9051-2), Gemini MV (GeoB 9067-1), Unnamed MV (9063-1), and Hesperides MV (GeoB 9021-1). Sediments consist mainly of gas-saturated homogeneous mud breccias with low organic carbon content (Table 1). Samples from Ginsburg MV were characterized by a distinct smell of petroleum. Gas hydrates, which have been previously recovered from various sites (Mazurenko et al., 2003; Pinheiro et al., 2003, 2005), were retrieved only at CAMV.

3.1. Sediment sampling

Gravity cores generally were taken after prior investigation with a video sled (OFOS—ocean floor observation system) and sampling of shallow surface sediments using a video-guided multi-corer (Niemann et al., 2006). The cores were segmented in pieces of 1 m and cut lengthwise in a cooled laboratory at about 6 °C. Sediment samples for pore water and gas analyses were collected within 1–2 h after retrieval. Although it is a well-known fact that most (up to 95%) of the light hydrocarbon gases are lost during core recovery, the remaining methane is highly enriched above background values and can be used for reliable flux calculations (Niewöhner et al., 1998) and isotope analyses (Wallace et al., 2000). Pore waters were squeezed using a pressure filtration system at pressures up to 5 bar and filtered through 0.45 lm cellulose acetate membrane filters. Pore water samples were then immediately analysed onboard or sub-sampled for subsequent analysis. Sediment samples for pore water hydrocarbon gas analysis were extruded and disaggregated in sealed 35 ml vials containing 10 ml of a 10%-KCl solution to stop all microbial activity (Bowes and Hornibrook, 2006).

3.2. Pore water analysis

Onboard analyses were performed for the most sensitive parameters (alkalinity, H_2S, and NH_4) immediately after

Table 1
Location of the gravity cores and general characteristics of the MV study sites

Site	Core NumberGeoB	Latitude (°N)	Longitude (°W)	Water depth (m)	Average TOC (wt%)	Bottom water T (°C)
Captain	9041-1	35°39.7′	7°19.97′	1316	0.35	9.3
Arutyunov MV	9072-1	35°39.71′	7°19.95′	1321	0.34	
Hesperides MV	9021-1	36°10.99′	7°18.38′	701	0.22	12
Bonjardim MV	9051-2	35°27.61′	9°00.03′	3087	0.27	3.1
Ginsburg MV	9061-1	35°22.42′	7°05.29′	912	0.29	10
No Name MV	9063-1	35°21.99′	6°51.92′	598	0.36	13[a]
Gemini MV	9067-1	35°16.92′	6°45.47′	435	0.30	15[a]

[a] Estimated.

pore water separation. Total alkalinity was determined by titration (Ivanenkov and Lyakhin, 1978), whereas dissolved NH_4 and total H_2S were determined using standard photometric procedures (Grasshoff et al., 1983). The remaining pore waters were later analysed in the shore-based laboratory at IFM-GEOMAR for dissolved anions (SO_4^{2-}, Cl^-, I^-, Br^-) and cations (Na^+, K^+, Li^+, Mg^{2+}, Ca^{2+}, Sr^{2+}, Ba^{2+}, B (boric acid), Si (silicic acid)) using ion chromatography and optical ICP, respectively. Subsamples for dissolved element analyses (by ICP) were acidified immediately after pore water squeezing to prevent any precipitation of minerals due to depressurisation and degassing.

Sediment porosity was calculated from the water content (weighing fresh and freeze-dried samples) assuming a dry solid density of 2.65 g cm^{-3}. Total organic carbon was determined by flash combustion of freeze-dried and ground using a Carlo Erba element analyser (NA1500) with a relative standard deviation of about 1% for replicate measurements. All analytical procedures applied on board and at IFM-GEOMAR laboratories are described elsewhere (Luff and Wallmann, 2003; Aloisi et al., 2004a) and documented in detail at http://www.ifm-geomar.de/index.php?id=mg_analytik& L=.

Strontium isotopes were measured by thermal ionisation mass spectrometry (TRITON at IFM-GEOMAR) after Sr separation via ion exchange chromatography using a Sr-specific resin. The average $^{87}Sr/^{86}Sr$ value for NBS 987 run during this study ($n = 12$) was 0.710249 ± 0.000020 (2σ). Stable oxygen and hydrogen isotope composition of pore waters were measured by mass spectrometry at the GCA Laboratory in Sehnde (Germany) with a precision of 0.3‰ (oxygen) and 3.1‰ (hydrogen) using lab-internal, IAEA-calibrated standards (SLW: $\delta^{18}O = -8.35‰$ V-SMOW, $\delta D = -58.4‰$ V-SMOW; GRW: $\delta^{18}O = -33.59‰$ V-SMOW, $\delta D = -258.2‰$ V-SMOW).

3.3. Gas analysis

Light hydrocarbon gases were stripped from samples onboard by agitation of sediment in vials followed by an equilibration period of 48 h. Headspace gas was removed and stored for transport by injection into crimp-top vials previously filled with a pH ~ 1, 10% KCl solution. Light hydrocarbon gas abundances were measured using a Varian 3400 gas chromatograph (GC) equipped with a PLOT Q capillary column (0.32 mm × 30 m) and a flame ionisation detector (FID). Calibration standards for methane consisted of a range of BOC (UK) alpha-gravimetric mixtures and for C_2 to C_6 homologues a range of SCOTTY (UK) standards.

Analyses of $^{13}C/^{12}C$ ratios in CH_4 and C_2H_6 were conducted by GC–combustion isotope ratio mass spectrometry (GC-C-IRMS) at Bristol University using a Thermoelectron XP mass spectrometer. Light hydrocarbon gases were separated on a PLOT Q capillary column (0.32 mm × 30 m) and combusted to CO_2 at 1000 °C in a ceramic reactor containing Cu and Pt wires. A high purity blend of 1% O_2 in helium was fed into the reactor at 0.2 ml min^{-1} to ensure complete combustion. Calibration standards consisted of BOC (UK) alpha-gravimetric gas mixtures that had been analysed for $\delta^{13}C$ at external laboratories and a $\delta^{13}C$–CO_2 gas standard from Oztech Corporation (USA). Stable isotope ratios are reported in the standard delta (δ) notation in units of permil (‰) relative to Vienna Pee Dee Belemnite (VPDB).

3.4. Geochemical modelling

Rates of upward fluid flow, pore water mixing and AOM were determined by applying a reactive transport model running on Mathematica® Version 5.0 (Schmidt et al., 2005). The model considers molecular diffusion and advection of dissolved SO_4, CH_4, Cl, and B. We applied the general differential equation:

$$\phi \cdot \frac{\partial[C]}{\partial t} = \partial\left(\frac{\phi \cdot D_{\text{sed}} \cdot \frac{\partial[C]}{\partial x}}{\partial x}\right) - \phi \cdot v \cdot \frac{\partial[C]}{\partial x} - \phi \cdot R_{\text{AOM}} - \phi \cdot \alpha(x) \cdot (C(x) - C(0)), \quad (1)$$

where t is time (yr), x is sediment depth (cm), $[C]$ is the concentration of the dissolved pore water species (mmol dm^{-3}), D_{sed} is the diffusion coefficient in the sediments ($cm^2\ yr^{-1}$; corrected for tortuosity; (Boudreau, 1997), ϕ is the sediment porosity (unitless), v is the velocity of upward fluid flow (cm yr^{-1}), R_{AOM} is the rate of AOM (in μmol $dm^{-3}\ yr^{-1}$), $\alpha(x)$ is the depth-dependent pore water-mixing coefficient (yr^{-1}), and $(C(x) - C(0))$ is the difference between the concentration at any depth and in seawater.

The rate of AOM is calculated as:

$$R_{\text{AOM}} = k_{\text{AOM}} \cdot [SO_4] \cdot [CH_4], \quad (2)$$

where k_{AOM} is the rate constant ($dm^3\ mmol^{-1}\ yr^{-1}$).

Sediment porosity changes with depth due to sediment compaction. The depth profile is approximated by fitting the measured porosity data with:

$$\phi = (\phi_{\text{top}} - \phi_{\text{bot}}) * \text{Exp}(-\text{const} \cdot x) + \phi_{\text{bot}}, \quad (3)$$

where ϕ_{bot} and ϕ_{top} are the porosity at the base of each core and at the sediment surface, and const is the attenuation coefficient for the exponential decrease of porosity with depth.

At most of the sites surficial mixing of seawater into the sediment is observed within the first meter of the sediment. This process can be identified by unusually weak gradients in the upper part of pore water profiles and seems to be common in the vicinity of cold seeps. It is likely caused by density differences (inducing convection cells) between upward flowing fluid and seawater or by flow effects around morphological elevations (e.g. Henry et al., 1996; Schmidt et al., 2005; Haese et al., 2006). For the simulation of this fluid-mixing process a rate law formulation with a depth-dependent mixing coefficient has been applied:

$$\alpha(x) = \frac{\alpha'}{(1 + \mathrm{Exp}[(x - x_{\mathrm{mix}})/k]}, \quad (4)$$

where α' is the pore water-mixing coefficient (yr^{-1}), x_{mix} is the depth of the mixed layer (in cm), and k determines the thickness of the transition layer between the mixed and the non-mixed proportion of the sediment column (in cm).

Boundary conditions were defined for the sediment surface (0 cm) and the base of each respective core. The model was run to steady state beginning from arbitrary initial conditions. The upward flow and mixing rates were determined by fitting the model to the measured pore water geochemical data.

4. Results

4.1. Fluid geochemistry

4.1.1. Major ions

Concentration–depth plots of major ions for all study sites are shown in Fig. 2a and b. Apart from Hesperides MV pore waters generally become depleted in SO_4 within 30–300 cm below the sediment surface, followed by an increase in CH_4 below the SO_4–CH_4 transition (AOM) zone (Fig. 2a). In cores 9072-1 (CAMV) and 9061-1 (Ginsburg MV) SO_4 is present even below the AOM which will be discussed in more detail in Sections 5.1 and 5.2.2 Ca is

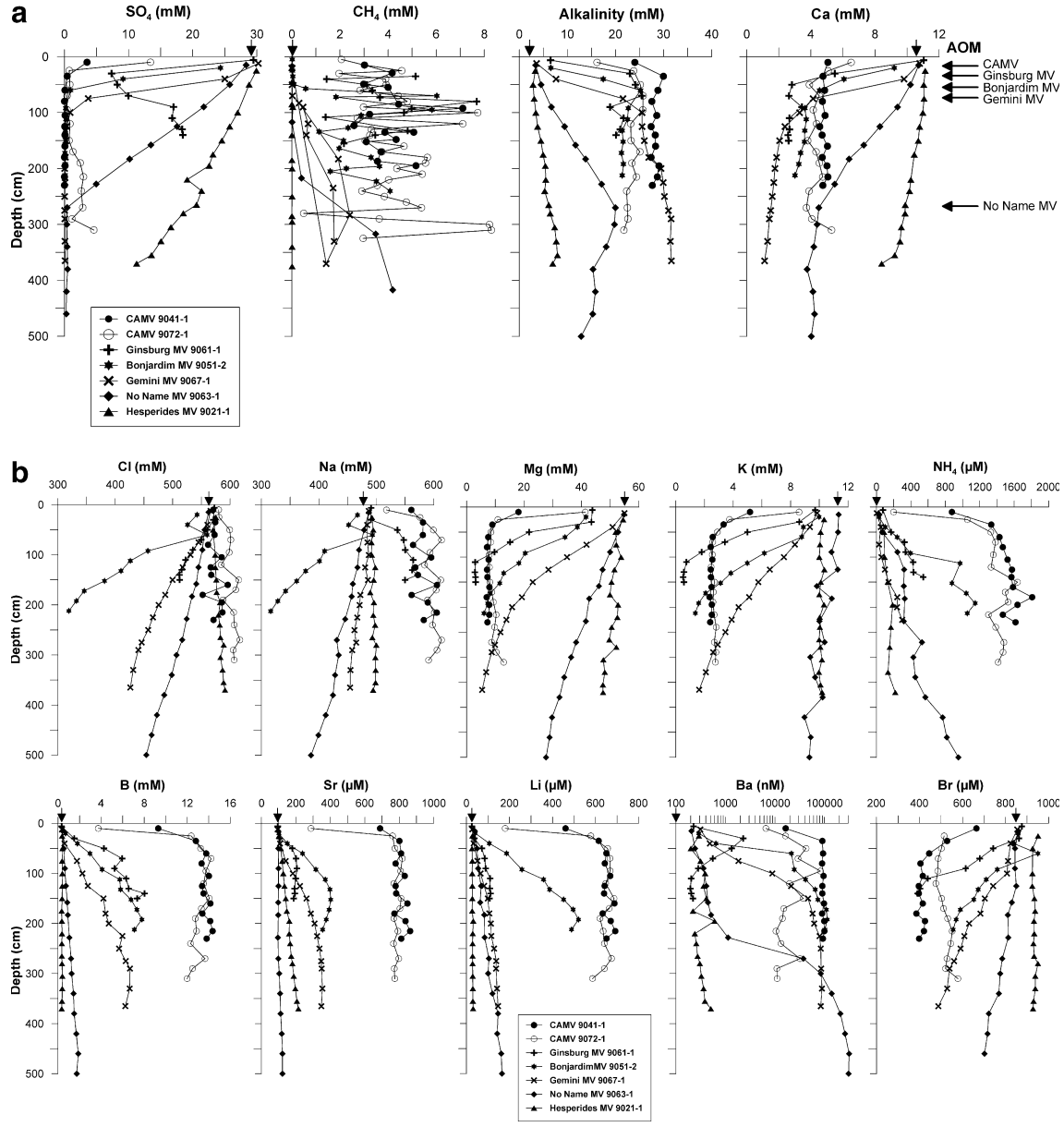

Fig. 2. (a) Pore water profiles of SO_4, CH_4, alkalinity, and Ca at all investigated sites. Vertical arrows indicate seawater values. Horizontal arrows indicate depth of AOM. (b) Pore water profiles of various elements at all investigated sites. Vertical arrows indicate seawater values.

generally depleted, accompanied by a simultaneous increase in alkalinity, from the AOM zone to the base of the cores at all sites (Fig. 2a). Although significant differences exist between the sites, there is a general decrease in Mg, K, and Br as well as an increase in Sr, Li, B, Ba, and NH_4 concentrations (Fig. 2b). The behaviour of Na and Cl is not uniform. Whereas Cl-concentrations of the fluids at CAMV and Hesperides MV are slightly enriched with respect to seawater, Cl is depleted at all other sites. The same trends are observed for Na with the exception of Ginsburg MV where Na and Cl show opposite trends with depth. These major characteristics are summarized in Table 2.

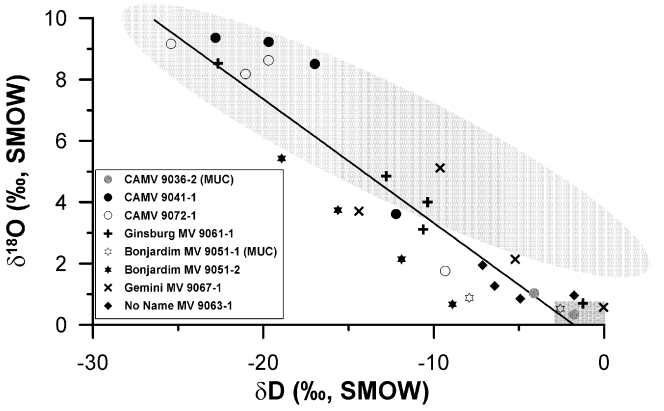

Fig. 3. δD vs. $\delta^{18}O$–H_2O values from various core depths at all sampled sites with exception of Hesperides MV. Additional surface samples from two multicorer cores at CAMV (9036-2) and Bonjardim MV (9051-1) are included. The observed negative trend clearly indicates clay mineral dehydration as the major fluid source. In general, the lowermost samples in each core show the strongest enrichment in $\delta^{18}O$ and depletion in δD; closer to the sediment–water interface dilution by seawater is overprinting the fluid signature. The shaded ellipse corresponds to data reported by (Dählmann and De Lange, 2003) from eastern Mediterranean MVs. The shaded rectangle indicates the composition of seawater.

4.1.2. Isotope data

Pore water samples from various depths in each core have been used to characterize the stable oxygen- and hydrogen-isotope systematics of the fluids. The results are summarized in a $\delta^{18}O$–δD plot (Fig. 3), which shows a clear negative trend. Usually, the deepest sample from each core shows the strongest deviation from seawater composition. Samples from different depths of CAMV cores (9041-1, 9072-1) plot in the upper left panel of Fig. 3, indicating the uniformity of fluid composition and a lack of dilution by seawater. For comparison, the field of $\delta^{18}O$–δD data from eastern Mediterranean mud volcanoes (Dählmann and De Lange, 2003) has been included in Fig. 3. The largest offset from seawater composition occurs at Captain Arutyunov and Ginsburg MVs.

One sample from the base of each core from Captain Arutyunov, Ginsburg, and Bonjardim MVs has been used for determination of $^{87}Sr/^{86}Sr$ ratios. The results (Fig. 4) show that fluids from CAMV clearly contain more radiogenic Sr than Ginsburg and Bonjardim MVs.

4.2. Dissolved hydrocarbon gases

The abundances of dissolved methane to pentane, and the $\delta^{13}C$ values of methane and its homologues were measured to assess the origin of light hydrocarbon gases in MV fluids. In spite of considerable loss in concentration during core recovery, the measured methane concentrations are still highly elevated above seawater values and appropriately reflect the in situ trend in shallow sediment layers (Fig. 2a). In fact, investigations by Wallace et al. (2000) did not show systematic deviations between the $\delta^{13}C$-values of methane from standard (degassed) and pressurized cores, implying that fractionation due to degassing is negligible. The overall results are summarized in Table 3. Gases at Bonjardim and Ginsburg MVs appear to possess clearly thermogenic signatures, exhibiting low $CH_4/(C_2H_6 + C_3H_8)$ ratios and ^{13}C-enriched CH_4 and C_2H_6. Gas in pore fluids at CAMV is unusual because it has

Table 2
Overview of element enrichments (+) and depletions (−) with respect to seawater at the study sites

Parameter	CAMV	Hesperides MV	Bonjardim MV	Ginsburg MV	Gemini MV	No Name MV
Na	+	+	−	+	−	−
Cl	+	+	−	−	−	
Ca	−	(−)	−	−	−	−
Mg	−	−	−	−	−	−
K	−	o	−	−	−	−
Sr	+++	+	+	++	+	o
Li	+++	o	+++	+	+	+
B	+++	o	++	++	++	+
Br	−	o	−	−	−	−
NH_4	++	+	+	+	+	+
SO_4 (at depth)	o/+	AOM not reached	o	++	o	o
Ba	+	(+)	+	(+)	+	+
CH_4	+	(+)	+	+	+	+

Slight changes are indicated parentheses and changes by 'o'. For Sr, Li, and B, a more differentiated scheme is provided in order to more clearly portray differences in fluid chemistry.

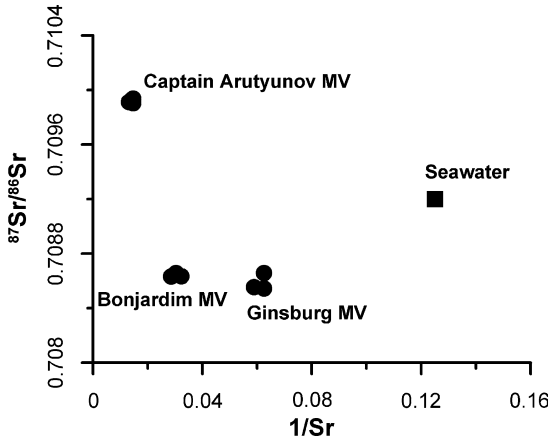

Fig. 4. $^{87}Sr/^{86}Sr$ systematics of end member pore fluids from Captain Arutyunov, Ginsburg, and Bonjardim MVs. Pore fluids at CAMV contain more radiogenic Sr compared to seawater, whereas Ginsburg and Bonjardim MVs are affected by less radiogenic sources.

a high $CH_4/(C_2H_6 + C_3H_8)$ ratio and also relatively positive $\delta^{13}C–CH_4$ values.

5. Discussion

5.1. Fluid advection and mixing processes

The purity of the geochemical signature of the pore water is dependent on the overall advection rate of the upward migrating fluid and irrigation processes in the subsurface sediments. In order to derive quantitatively well-constrained estimates of the advection rate we performed numerical model runs with conservative (Cl, B) and reacting parameters (SO_4, CH_4). Under environmental conditions met in the uppermost surface layers, Cl and B can be considered as geochemically conservative and hence their depth profiles provide useful parameters to estimate upward rates of fluid flow (Martin et al., 1996; Aloisi et al., 2004a; Haese et al., 2006). The consistency of flux rates can be checked by simultaneously modelling reactive solutes (e.g., SO_4 and CH_4). In addition, the transition zone of SO_4 and CH_4 (AOM; Fig. 2a) is a perfect measure of the depth of near-surface mixing and oxidation processes in the vicinity of a vent site. A more detailed discussion of AOM at Gulf of Cadiz MVs is given in Niemann et al. (2006).

All model parameters used to produce the fitted curves shown in Fig. 5 are summarized in Table 4. In general, good and internally consistent curve fits for Cl, B, and SO_4 could be produced for all sites. The scatter in Cl-profiles below 50 cm bsf at CAMV is attributed to the occurrence of gas hydrate at this site, and hence the maximum Cl-concentration measured in each of the cores has been used as the lower boundary (maximum) concentration in the model. In these cases, B is a more reliable parameter because pore water concentrations are less affected by the presence of gas hydrates due to the high concentration difference between seawater and MV pore fluid. The location of the AOM zone and the resulting reaction rates in the

Table 3
Summary of end member gas geochemistry data for selected MV sites in the Gulf of Cadiz

Site	Core	CH_4 (mM)	$\delta^{13}C–CH_4$ (‰)	$\delta^{13}C–C_2H_6$ (‰)	$\delta^{13}C–C_3H_8$ (‰)	$\delta^{13}i$-C–C_4H_{10} (‰)	$\delta^{13}n$-C–C_4H_{10} (‰)	$C_1/(C_2 + C_3)$
Hesperides MV	GeoB 9021	$8 \pm 2\ 10^{-3}$ ($n = 5$)	n.a.	n.a.	—	—	—	—
No Name MV	GeoB 9063	n.a.	n.a.	n.a.	—	—	—	—
Bonjardim MV	GeoB 9051	2.9 ± 1.3 ($n = 12$)	-49.6 ± 0.7 ($n = 10$)	-28.1 ± 0.1 ($n = 4$)	-24.6 ± 0.4 ($n = 4$)	-26.7 ± 0.8 ($n = 3$)	-23.8 ± 0.4 ($n = 4$)	14 ± 3 ($n = 10$)
Ginsburg MV	GeoB 9061	4.2 ± 2.1 ($n = 7$)	-40.9 ± 0.4 ($n = 11$)	-22.5 ($n = 1$)	-22.1 ($n = 1$)	-24.1 ($n = 1$)	—	40 ± 14 ($n = 11$)
CAMV	GeoB 9041	4.2 ± 1.3 ($n = 10$)	-48.4 ± 0.3 ($n = 15$)	—	—	—	—	1020 ± 302 ($n = 15$)
CAMV	GeoB 9072	4.5 ± 1.8 ($n = 26$)	-48.3 ± 1.5 ($n = 32$)	—	—	—	—	1125 ± 510 ($n = 32$)
CAMV (gas hydrates)	GeoB 9036	48.9 ± 7.4 %v ($n = 3$)	-52.0 ± 0.4 ($n = 3$)	-24.0 ($n = 1$)	—	—	—	852 ± 145 ($n = 3$)

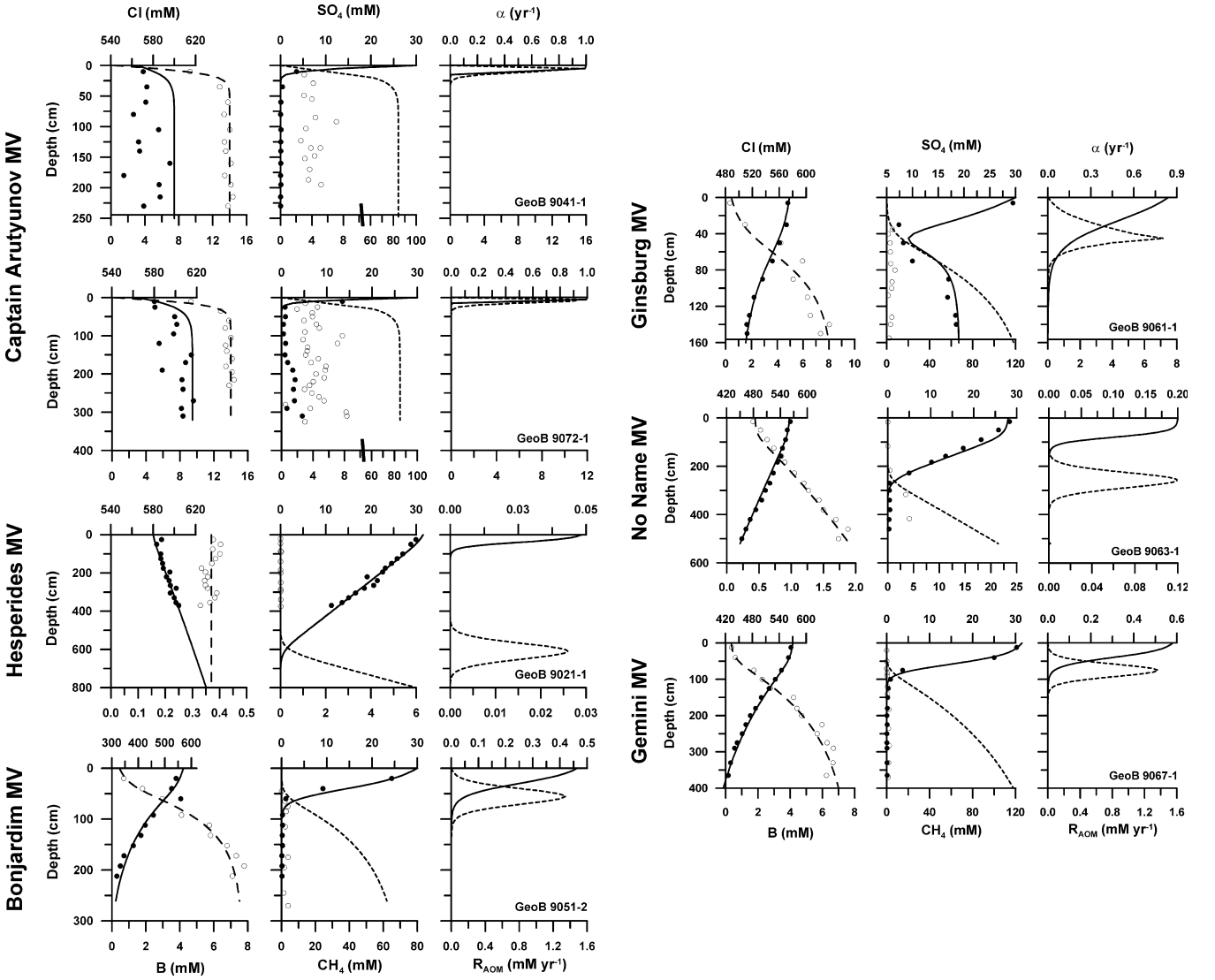

Fig. 5. Results of numerical modelling (solid lines: Cl, SO_4, α; dashed lines: B and CH_4, R_{AOM}) for the various cores investigated in this study (core reference in the right-hand plots). Measured data are represented by closed circles for Cl and SO_4 and open circles for B and CH_4, respectively. Note the different horizontal scales in the various plots.

model are strongly dependent on methane concentrations prescribed at the lower boundary (CH_4(B)). With the exceptions of Hesperides and No Name MVs (GeoB 9021-1 and GeoB9063-1, respectively), the CH_4(B) concentration corresponds to (CAMV; GeoB9041 and GeoB9072), or is slightly below the ambient methane solubility with respect to gas hydrate stability (Tishchenko et al., 2005). As outlined above (Section 3.1), the large discrepancy between measured and modelled concentrations is due to the significant decrease of methane solubility and degassing during core recovery. Hence, the MV fluids are probably saturated with CH_4 at all sites, except at Hesperides and No Name MVs, where upward fluid flow rates are low and SO_4 penetrates deeply into the sediment so that saturation levels of dissolved CH_4 cannot be expected within the core depth.

Shallow near-surface gradients of all solutes are explained by active admixing of bottom water, which seems to be a typical feature at cold vents (Henry et al., 1996; Schmidt et al., 2005; Haese et al., 2006). Due to the elevated advective flow velocities, the mixing zone is very thin in the CAMV cores and only resolved by multicorer sampling (Niemann et al., 2006). Overall, flux rates decrease from CAMV to Hesperides MV in the order listed in Table 4 (from left to right). This decrease is in accordance with the preservation of the fluid signal: the higher the advective flux, the lower is the admixing of seawater and hence the purer the fluid composition. Effective diffusive exchange between pore fluids and bottom water is limited to the uppermost centimetres of the sediment when the flow rates exceed a threshold of some centimetres per year (Luff and Wallmann, 2003).

The unusual situation of high sulphate levels in rising fluids at Ginsburg MV required inhibition of AOM in the model below the maximum mixing depth in order to produce consistent results. The coexistence of SO_4 and

Table 4
Properties and boundary conditions used for numerical modelling

Parameter	Symbol	Core No.							
		Captain Arutyunov MV		Ginsburg MV (9061-1)	Bonjardim MV (9051-2)	Gemini MV (9067-1)	No Name MV (9063-1)	Hesperides MV (9021-1)
		9041-1	9072-1					
Column length (cm)		250	320	160	260	400	520	800
Upward fluid flow (cm yr^{-1})	v	15	10	3	1.3	0.6	0.1	(<)0.05
Porosity (sediment surface)	ϕ_{top}	0.65	0.65	0.65	0.65	0.64	0.7	0.62
Porosity (lower boundary)	ϕ_{bot}	0.57	0.62	0.57	0.57	0.52	0.57	0.5
Attenuation coefficient (cm^{-1})	const	0.05	0.05	0.05	0.05	0.02	0.05	0.02
Rate constant of AOM (dm^3 mmol^{-1} yr^{-1})	k_{AOM}	0.1	0.1	0.5	0.1	0.1	0.1	0.1
Mixing coefficient (yr^{-1})	α'	—	—	2.5	0.5	0.6	0.2	0.05
Depth of the mixed layer (cm)	x_{mix}	10	10	20	30	40	80	40
Mixed layer coefficient (cm)	k	1	1	12	12	12	12	12
Chloride (sediment surface) (mmol dm^{-3})	Cl(0)	565	565	575	570	570	560	580
Chloride (lower boundary) (mmol dm^{-3})	Cl(B)	600	607	510	315	415	450	630
Boron (sediment surface) (mmol dm^{-3})	B(0)	0.4	0.4	0.44	0.44	0.34	0.44	0.37
Boron (lower boundary) (mmol dm^{-3})	B(B)	14	14	8	7.5	7	1.9	0.37
Sulphate (sediment surface) (mmol dm^{-3})	$SO_4(0)$	30	30	30	30	31.5	28	31.5
Sulphate (lower boundary) (mmol dm^{-3})	$SO_4(B)$	0	0	0	0	0	0	0
Methane (sediment surface) (mmol dm^{-3})	$CH_4(0)$	0	0	0	0	0	0	0
Methane (lower boundary) (mmol dm^{-3})	$CH_4(B)$	85	85	130	62	120	21.4	6

CH_4 in the deeper part of the core further indicates that AOM must be attenuated along the flow path, because microbes may fail to find favourable growth conditions within the flowing medium.

Seawater intrusion at Ginsburg MV cannot account for the SO_4 enrichment in MV fluids as they are almost entirely depleted of K and Mg (Fig. 2). We suspect that high SO_4 levels are caused by dissolution of anhydrite or gypsum at greater depth (see also Section 5.2.2). In contrast to Ginsburg MV (GeoB9061-1), the very slight increase of sulphate at CAMV (GeoB 9072-1) can be readily attributed to a <10% admixing of seawater as it is accompanied by a similar increase of K and Mg and an obvious decrease of Ba-levels (Fig. 2). These hypotheses are further substantiated by the calculation of saturation levels (Ω) for barite (using average Ba and SO_4 concentrations of the cores 9072-1 and 9061-1 below the AOM and the solubility constant for barite in seawater provided by (Aloisi et al., 2004b) which indicate highly supersaturated fluids at CAMV ($\Omega > 3$) and undersaturated fluids ($\Omega < 0.5$) at Ginsburg MV. Since precipitation kinetics of barite are relatively slow (Aloisi et al., 2004b) supersaturation is indicative of a non-equilibrated system (recent seawater admixing into Ba-rich fluid) whereas the undersaturated fluids may have had sufficient time for equilibration due to the deep source of SO_4.

5.2. Origin of the fluids

5.2.1. Evidence for clay mineral dehydration

As demonstrated by numerical modelling, the most active sites of fluid advection are GeoB 9041-1 and 9072-1 located at CAMV. The compilation δD and $\delta^{18}O$ values of pore water samples from all investigated sites (Fig. 3) reveals a clear negative correlation which is typical for water that has been released by clay mineral dehydration, most likely by the transformation of smectite to illite (Sheppard and Gilg, 1996; Dählmann and De Lange, 2003). This observation is in accordance with data from Mediterranean Ridge mud volcanoes (Fig. 3) and earlier observations at Yuma and Ginsburg MVs in the Gulf of Cadiz (Mazurenko et al., 2003), although interpreted differently by the latter authors. The major temperature field for this process ranges between 60 and 150 °C (Freed and Peacor, 1989; Chan and Kastner, 2000). Applying an average geothermal gradient of 30 °C per km, the upper limit of formation depth would be approximately 5 km bsf, which comprises the lower sedimentary units deposited on basement rocks (Medialdea et al., 2004).

Due to the complex stratigraphic and tectonic development in this area it is difficult to unambiguously identify the "source rocks". Potential sedimentary sources to be considered belong to the Sub-Betic and other Mesozoic units as well as the so-called Allochthonous Unit of the Gulf of Cadiz (AUGC) comprising mainly Tertiary and Mesozoic shales and marls, which are overlain by up to 1 km of Plio-Quaternary hemipelagic sediments and pene-

trated by deep-reaching faults (Medialdea et al., 2004; Pinheiro et al., 2005). An abundance of smectite has been reported in sediments affected by terrigeneous input (Chamley, 1989; Reicherter and Pletsch, 2000). However, the clear stable isotopes signal (Fig. 3) strongly suggests that the release of freshwater at greater depth is the quantitatively dominant process of fluid formation in this area. The upward migration of the overpressured fluids occurs under tectonic control, causing the liquefaction of sediments and the formation of mud volcanoes, which appear to be located along deep strike–slip faults and thrusts, or at fault intersections (Pinheiro et al., 2005; Fig. 1).

5.2.2. *Overprinting of the fluid signature by secondary processes*

In principle, the release of mineral-bound water results in a general freshening of pore fluids reflected by decreased concentrations of Na and Cl, and other major solutes (Fig. 2). Such a dilution trend is also depicted in Fig. 6. However, deviations from the mixing line between seawater and fluid suggest the occurrence of additional processes leading to coeval and subsequent overprinting of the fluid composition. Whereas Na is relatively enriched with respect to Cl, Mg, and K are considerably depleted. Similar observations have been reported from mud volcano sites at different continental margins around the world (Martin et al., 1996; Aloisi et al., 2004a; Godon et al., 2004).

Relative Na enrichments over Cl are thought to be a direct consequence of the transformation of smectite to illite where Na is released into solution. The increase in Na is then a simple function of the relative amount of Na to H_2O in the smectite. This, however, is difficult to estimate since the Na–H_2O ratio of natural smectites is a quite variable factor. Considering, for the moment, only those sites where the pore water chlorinity indicates freshening, there is a clear trend in Na increase in the order: No Name MV (~seawater dilution) < Bonjardim MV < Gemini MV < Ginsburg MV. In simple terms, this would mean that the Na content in the original smectite would have shown an increase in the same order of sites. This relation is more clearly illustrated in Fig. 7. Assuming that the observed dilutions with respect to seawater are caused by "dissolution" of a typical smectite (montmorillonite) containing 15 wt% of water (Sheppard and Gilg, 1996), the relative amount of Na in the smectites can be calculated by matching the observed endmember concentration in each core. In the same order of MVs as given above this would be 0.004, 0.007, 0.028, and 0.12 mol Na per mol of smectite.

Specifically for Ginsburg MV these observations are, however, inconsistent with isotope data (Fig. 3) and modelled advection rates (Fig. 5 and Table 4) as, in theory, the degree of freshening should be in accordance with the isotope signal and with the rate of fluid flow. Hence, this obvious contradiction at Ginsburg MV suggests that other processes release Na into solution, preferentially without altering the isotope ratios of oxygen and hydrogen.

The incongruent dissolution of Na-feldspars (albite to kaolinite; Eq. (5)) could be considered as one possibility,

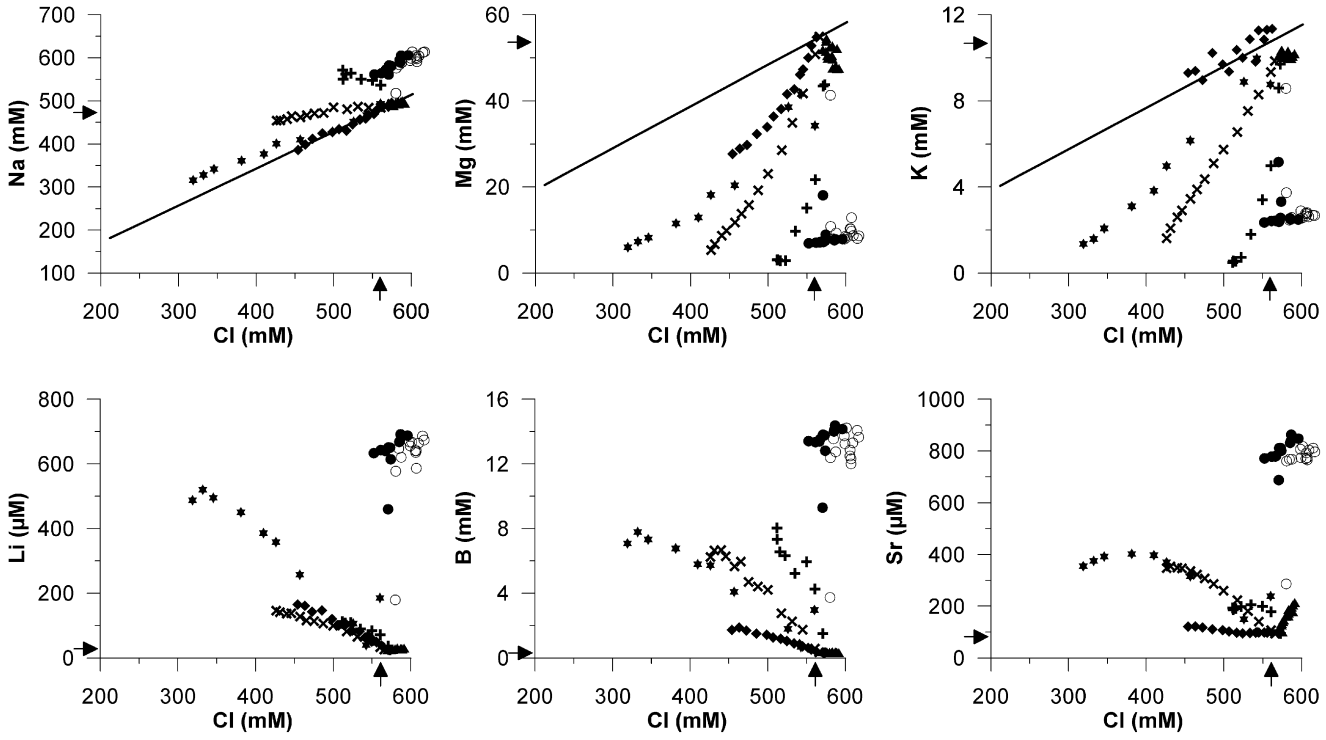

Fig. 6. Fluid property plots of Cl vs. Na, Mg, K (upper panel) and Li, B, Sr (lower panel). See Fig. 2 for symbols. The solid lines in the upper panel plots indicate freshening (dilution) of seawater with constant element ratio. Arrows indicate seawater values.

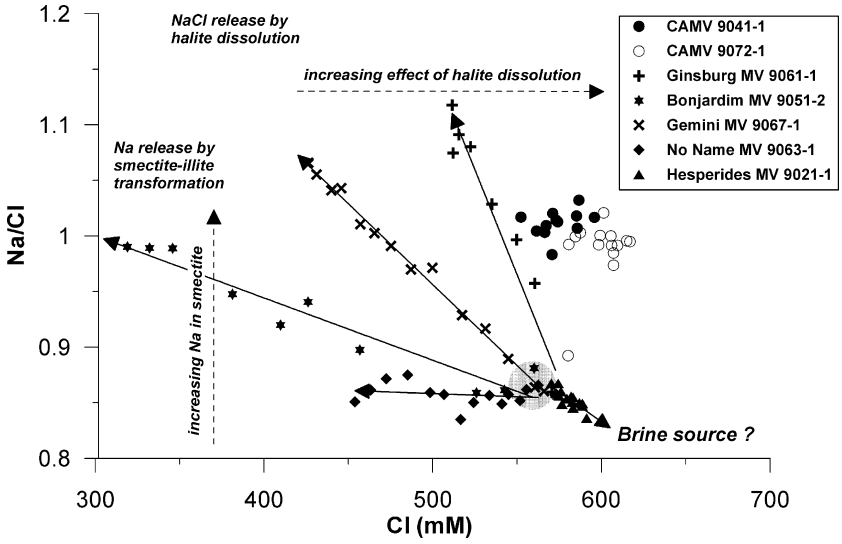

Fig. 7. Plot of Cl vs. Na/Cl indicating potential processes overprinting the primary composition of the fluids at various MV sites.

which, at the same time, could additionally account for increased levels of alkalinity.

$$2NaAlSi_3O_8 + 2H_2CO_3 + 9H_2O \Rightarrow 2Na^+ + 2(HCO_3)^- + 4H_4SiO_4 + Al_2Si_2O_5(OH)_4 \quad (5)$$

Unfortunately, this process would theoretically counteract the observed δD trend (Fig. 3) and the freshening of the fluid as it consumes considerable amounts of water.

However, we believe that all observations discussed above can be consistently explained by the simple addition of NaCl (from leaching of halite) to a freshened fluid. In contrast to the sites exhibiting pore water freshening, fluids from Captain Arutyunov are enriched in both Na and Cl (Fig. 7) and the approximately constant Na/Cl ratio of 1 at CAMV indicates the dissolution of halite (e.g. Bernasconi, 1999). However, typical brines resulting from leaching of halite usually exhibit much higher concentrations of NaCl. This implies that the measured concentration of 600 mM can only be explained by a mild leaching of NaCl. Adding some NaCl to seawater would, however, not yield a fluid with a Na/Cl ratio of 1. Taking into account that this site exhibits the highest advection rates in combination with the clearest δD and $\delta^{18}O$ signal of all sites within the study area, we may conclude that a strongly freshened fluid is dissolving halite at depth. For such a low salinity fluid only slight additions of Na released during clay mineral transformation are needed in order to shift the NaCl ratio from 0.87 (in seawater) to about 1. In the same way, the opposite trends at Ginsburg MV (Cl-depletion and Na-enrichment) can be sufficiently explained, by simply leaching less NaCl by a freshened, but slightly more Na-enriched original fluid. In order to obtain an approximation to the original Cl concentration at Ginsburg MV and CAMV we used the obvious relation between Cl and $\delta^{18}O$ at those sites, which are not affected by halite dissolution. As data from Gemini MV may also indicate some offset, we only used seawater and concentrations from No Name and Bonjardim MVs to produce the exponential fit shown in Fig. 8. From this relation we can deduce that original Cl concentrations of freshened fluids at may have been between 250 mM (Ginsburg MV) and ~230 mM (CAMV) and about 270–370 mM Cl have been added by leaching of halite, respectively. In addition, we (re)-calculated the molar Na fractions of smectites that would be required to produce the measured Na/Cl ratios at Gemini MV (0.02), Ginsburg MV (0.012), and CAMV (0.075). The considerably decreased Na fractions at Gemini and Ginsburg MVs further support the hypothesis since they imply less regional variability of natural smectites in the

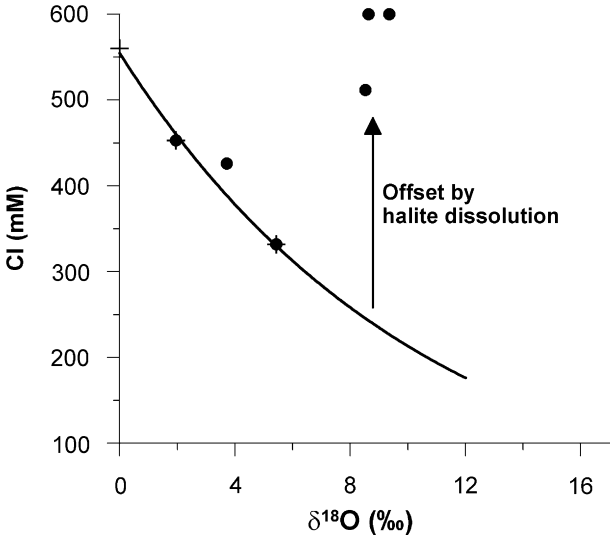

Fig. 8. Reconstruction of original Cl concentrations from $\delta^{18}O$ values in the freshened fluid before overprinting by halite dissolution. The exponential fit function is obtained using values of seawater and the sites unaffected by halite dissolution (No Name MV, Bonjardim MV; $Cl = e^{(-0.0955 \cdot \delta^{18}O)} \cdot 554.37$). Arrow indicates offset created by halite dissolution at CAMV and Ginsburg MV.

working area. In addition, data from a very recent cruise by RV Merian in May 2006 revealed the unequivocal evidence for the existence of strongly saline brines in mud volcano fluids in the Gulf of Cadiz. Nearly NaCl-saturated and strongly SO_4-enriched (80 mM) have been reported from Mercator MV (some 30 km east of Ginsburg MV towards the Moroccan coast; M. Haeckel, pers. comm., RV Maria S. Merian cruise MSM01/3, 2006). As outlined in Section 5.1, elevated pore water SO_4 concentrations at Ginburg MV most likely result from leaching of gypsiferous clays and brecciae that generally cap deposition centres in the Gharb Basin (Maestro et al., 2003; Medialdea et al., 2004).

In contrast, slightly decreasing Na/Cl ratios at Hesperides MV (Fig. 7) may indicate evaporated seawater or residual brines as a potential source in Hesperides MV (e.g. (McCaffrey et al., 1987). However, low advection rates at Hesperides MV cause a weak geochemical signal and hence, this interpretation is more speculative and will not be discussed in more detail.

Mg and K are strongly depleted in pore fluids at all sites (with the exception of K in No Name MV fluids; Fig. 6). In principle, the level of depletion is a function of advection rates, where the greatest advection produces the largest composition offset from seawater. The most likely explanation for the K-depletion in MV fluids is its integration into illite during clay mineral transformation (Martin et al., 1996; Aloisi et al., 2004a; Godon et al., 2004). Moreover, K is considered to be a major factor controlling the kinetics of smectite to illite transformation and the lack of K may even cause incomplete reaction (Spinelli and Underwood, 2004; Cuadros, 2006). This case is strengthened by the strong correlation of K with either increasing $\delta^{18}O$, as depicted in Fig. 9, or with decreasing δD. In contrast, there is no correlation between Na and $\delta^{18}O$–H_2O values resulting from dissolution of halite affecting Na and Cl levels in pore water as outlined above.

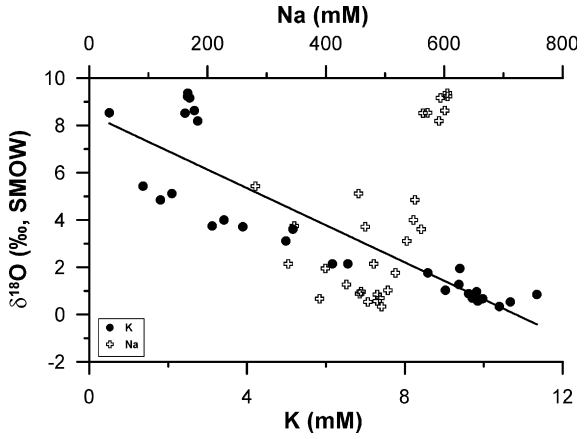

Fig. 9. Plot of K and Na vs. $\delta^{18}O$ demonstrating that the K-depletion is likely related to an early stage of fluid generation (formation of illite), whereas the scatter in Na indicates subsequent overprinting at various sites.

The depletion in Mg and Ca at all sites (Fig. 2) can be ascribed to carbonate precipitation at any depth below core penetration. Although calcium carbonate precipitation related to AOM can be assumed, Ca-depletion below the AOM zone is typical for all sites. Hence, low Ca concentrations controlled by high levels of alkalinity (generated by organic matter breakdown and submarine weathering processes) are an inherent feature of the upward migrating fluids before reaching the surface sediments. The slight curvature of the Mg concentration depth profile (Fig. 2) or in the Mg vs. Cl plot shown in Fig. 6 does indicate the occurrence of co-precipitation of authigenic Mg-calcite related to AOM, although low Mg-levels are most probably largely controlled by the dolomitisation of widespread Tertiary and Mesozoic carbonates (Maldonado et al., 1999; Medialdea et al., 2004) deeper within the mud volcanoes.

5.2.3. *High temperature imprint in the fluid signature*

The most obvious enrichments observed are those in B, Li, and Sr (Figs. 2 and 6). B- and Li-enriched fluids are well-known from numerous locations along active continental margins worldwide (You et al., 1993; Martin et al., 1996; Chan and Kastner, 2000; Haese et al., 2003; Aloisi et al., 2004a; Hensen et al., 2004) and may be primarily released from clay minerals (Brumsack and Zuleger, 1992). Under experimental conditions simulating hydrothermal alteration of hemipelagic sediments Li is enriched preferentially over B as temperatures increase above 150 °C (You et al., 1995; Chan et al., 1999; You and Gieskes, 2001). The B/Li ratio in the Gulf of Cadiz fluids is consistently >10; however, Li concentrations as high as 700 μM and B abundances up to 15 mM are amongst the highest levels reported to date from offshore cold seep environments (Aloisi et al., 2004a; Godon et al., 2004; Haese et al., 2006). Hence, the low ratios instead may be caused by different mechanisms of Li and B release or different source-rock potentials, rather than being an indicator of low temperature alteration. For comparison, vent fluids at the convergent margin off Costa Rica are thought to be derived from sources having temperatures up to 150 °C; here, only B, but no Li enrichments were detected (Hensen et al., 2004). Similar results are reported from freshened mud volcano fluids of the Mediterranean Ridge (De Lange and Brumsack, 1998; Haese et al., 2006; Haese, personal communication). In contrast, fluids detected along distinct fault zones at ODP site 1040 at the Costa Rica margin (Chan and Kastner, 2000) are similar in composition to the vent fluids but are enriched in Li up to 300 mM. This finding rather suggests that deep and shallow fluid systems at the Costa Rica convergent margin are less well connected and the transmission of any original high temperature signal may be affected by the amount of mixing with other fluids and various reactions occurring along the flow path. However, following the results of (You and Gieskes, 2001), we propose that Li-enrich-ments—at least above certain threshold value—are indica-

tive for geochemical reactions occurring at temperatures above 150 °C. This hypothesis is further strengthened by data from other vent locations: higher Li, but lower B values have been reported from MV fluids in the Black Sea (Aloisi et al., 2004a) and Barbados accretionary complex (Godon et al., 2004). Similar Li enrichments at the Peru convergent margin observed by Martin et al. (1991) have been ascribed to alteration of oceanic basement at moderate to high temperatures. Enrichments in B of up to 15 mM are atypical for hydrothermal fluids; hence such extreme levels must be caused by extensive leaching of sedimentary B. This may also include the release of lattice-bound B, which makes up a significant part of the sedimentary B reservoir and which is remobilised at temperatures of approximately 300 °C (You and Gieskes, 2001; Kopf et al., 2003).

Because Li is only highly enriched at Captain Arutyunov and Bonjardim MVs, but B-levels are elevated at all sites where advection rates exceed 0.1 cm yr^{-1} (Table 4 and Fig. 6) we hypothesize that the fluid, which is predominantly derived from clay mineral dehydration, has been subject to injection of basement derived fluids, which are likely Li-enriched and may additionally contribute to higher levels of B and Li from leaching of clays at temperatures >150 °C. Interestingly vent fluids from mid-ocean ridges buried beneath sedimentary cover (Von Damm et al., 1985, 2005) reach similar levels. This is illustrated by the compilation of Li and B concentrations of various hydrothermal and cold vent sites in Fig. 10. Low-temperature alteration sites (I) are characterised by high B/Li ratios and low (<100 μM) Li concentrations, high-temperature altered cold vent (II) and sediment covered hydrothermal vent sites (IV) show low B/Li ratios accompanied by high (>350 μM) Li concentrations, and hydrothermal vents at ridge crests (III) lack a significant B component revealing Li/B ratios <1. Thus, CAMV in particular may represent the cool end member of a hydrothermal injection system beneath a thick sedimentary cover, resulting in the enrichment of B versus Li (Chan et al., 1999). The fact that we do not observe typical hydrothermal signals, like K and Ca enrichments, can be ascribed to subsequent depletion by smectite-illite transformation and calcium carbonate precipitation, respectively. As discussed above, both processes are unambiguously occurring in the subsurface of the mud volcano sites and, moreover, the supply of K is well known to be limiting for the smectite-to-illite reaction (e.g. Boles and Franks, 1979; Cuadros, 2006). Overall, Mg depletions are also well in line with the impact of hydrothermal solutions, even though low Mg levels are also a likely result of dolomite precipitation.

This general hypothesis is supported by additional observations. For example, B and Li enrichments correlate generally with Sr suggesting a common release mechanism during fluid formation. Sr-enriched fluids are typically considered to result from carbonate recrystallisation, which may reduce the Sr content of carbonate minerals by as much as an order of magnitude (Morse and Mackenzie, 1990). Mesozoic and Tertiary carbonates are widespread in the Gulf of Cadiz and may provide potential Sr-sources at all sites investigated. However, analyses of $^{87}Sr/^{86}Sr$ ratios suggest that Sr originated from disparate fluid sources at the different MV sites (Fig. 4). Fluids at Bonjardim and Ginsburg MVs contain less-radiogenic Sr, which at Ginsburg MV (GeoB9061) may be related to dissolution of Tertiary and Cretaceous carbonates and evaporites (Burke et al., 1982; Banner, 2004) as suggested by the high sulphate levels at this site. However, because

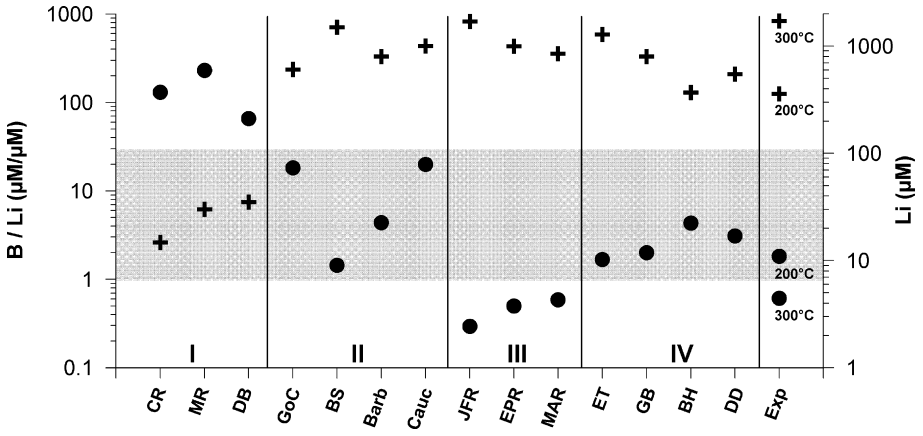

Fig. 10. Average B/Li ratios (dots) and Li concentrations (crosses) from selected cold vents (I, II), hydrothermal vents (III), sediment covered hydrothermal vents (IV), and hydrothermal experiments. There is a conspicuous similarity between fluids of fields II and IV, which are characterised by average Li/B ratios >1 (shaded rectangle) and corresponding high Li concentrations (>350 mM), implying that a high temperature imprint is preserved in certain cold vent areas. Data from hydrothermal experiments (Exp) at 200 and 300 °C (You and Gieskes, 2001) are presented for comparison. CR, Costa Rica (Hensen et al., 2004); MR, Mediterranean Ridge (De Lange and Brumsack, 1998; Haese et al., 2006); DB, Derugin Basin, Sea of Ochotsk (K. Wallmann, unpublished data); GoC, Gulf of Cadiz, average values of CAMV and Bonjardim MV (this study); BS, Dvurechenskii MV, Black Sea (Aloisi et al., 2004a); Barb, Barbados MVs (Dia et al., 1995; Godon et al., 2004); Cauc, Caucasian MVs (Kopf et al., 2003); JDF, Juan de Fuca Ridge; EPR, East Pacific Rise; MAR, Mid Atlantic Ridge (all Von Damm, 1990); ET, Escabana Trough; GB, Guaymas Basin; BH, Bent Hill, Middle Valley; DD, Dead Dog, Middle Valley (all Von Damm et al., 2005).

Bonjardim MV likely is underlain by oceanic crust (Gutscher, 2004; Medialdea et al., 2004) and Li is more enriched at this site, $^{87}Sr/^{86}Sr$ ratios may rather point to leaching of oceanic crust imprinting on the fluid composition. The radiogenic signature at CAMV suggests that significant interaction has occurred between fluids and continental crust material. This finding is supported by deep seismic studies, which have shown that the eastern part of the Gulf of Cadiz is underlain by thick continental crust covered by the Betic–Rifean Allochthonous Units (Gonzalez-Fernandez et al., 2001; Medialdea et al., 2004; Zeyen et al., 2005). As shown in Figs. 2 and 6, fluids from CAMV (and to some degree from Bonjardim MV also) exhibit a strong correlation between Li, B, and Sr and are offset from the other sites. Since Sr is also relatively enriched (with respect to seawater) in continental crust and terrigeneous sediments (shales), this finding supports the hypothesis of simultaneous "leaching" of these elements from clay minerals at moderate to high temperatures. Overall, the observations are consistent with data from the convergent margin off Chile where different $^{87}Sr/^{86}Sr$ ratios of Li-enriched fluids are interpreted to be caused by interaction with different crustal sources (Martin et al., 1991).

Likewise, the molecular and isotopic composition of light volatile hydrocarbon gases in expulsion fluids at CAMV is unusual. The gases have a clear thermogenic origin at Ginsburg and Bonjardim MVs (Table 3). The composition of CAMV gas also indicates a thermogenic origin, as shown by the stable carbon isotope signature of ethane in gas hydrates recovered at this site (Table 3). However, the high enrichment in methane cannot result from an admixture of migrated thermogenic gas and shallow microbial methane, due to very low microbial methanogenic activity in the shallow sediments (M. Nuzzo, unpublished data). This finding is in agreement with sediment TOC abundances that never exceed ~0.5% (Table 1) and generally low fluid concentrations of NH_4 and Br (Fig. 2b, Table 2; Martin et al., 1993). A catagenic origin of the methane expelled at CAMV is thus a more likely hypothesis, consistent with fluid geochemical indications for temperatures in excess of 150 °C. In this line of evidence, increased NH_4 concentrations at CAMV (Fig. 2) could be the result of the thermal alteration of organic material as reported from sediment covered hydrothermal vents (Thornton and Seyfried, 1987).

Expulsion of hydrothermally affected fluids at Bonjardim and Captain Arutyunov MVs, but not at Ginsburg MV is consistent with the locations of these edifices in different structural environments within the Gulf of Cadiz. Bonjardim and Captain Arutyunov MVs appear to be situated along major crustal strike–slip faults associated with the Africa/Eurasia Plate Boundary (Duarte et al., 2005), for which no evidence exists at Ginsburg MV (Fig. 1). It has indeed been shown that stress is released at strike–slip faults, thus focussing the expulsion of deep over-pressured fluids (Behrens, 1988; Tobin et al., 1993). The emplacement of Bonjardim and Captain Arutyunov MVs may actually be the result of intersecting strike–slip and thrust faults, which reduces compression and favours stress release by fluid advection (Chamot-Rooke et al., 2005). In contrast to Bonjardim and Captain Arutyunov MVs, fluids at Ginsburg MV likely are expulsed along extensional and thrust faults, similar to other MVs of the Moroccan margin (Van Rensbergen et al., 2005).

Theoretically, the continuous rise of warm fluids should be accompanied by an increased heat flow, which is not the case since average geothermal gradients at all sites are about 20–40 °C per km (Kopf and participants, 2004). However, comparatively low overall advection rates (Table 4) and insignificant emissions of methane into the overlying seawater (Niemann et al., 2006) are indicative for low present day expulsion rates. Variations in the activity of the mud volcanoes have been suggested earlier for this region (Pinheiro et al., 2003) and are in agreement with observations from various convergent margin settings where fluid advection along deep fault zones has been identified as a highly dynamic process which is subject to significant variations over time (e.g. Moore and Mascle, 1987; Martin et al., 1991; Saffer and Bekins, 1999; Hensen and Wallmann, 2005). Since a heat pulse equilibrates much faster in surface sediments compared to a geochemical signal as soon as the supply is disconnected, the present day geochemical composition of the fluids may be represent an imprint of the latest fluid pulse.

6. Conclusions

Fluid geochemistry at MVs in the Gulf of Cadiz indicates that major fluid formation and overpressuring is caused by clay mineral dehydration at several kilometres depth and temperatures of up to 150 °C, which is in agreement with the occurrence of thermogenic methane and similar observations at numerous cold vent areas worldwide (e.g. Martin et al., 1996; Dählmann and De Lange, 2003; Hensen et al., 2004). Quantitatively, the fluid composition can be largely explained by the transformation of smectite to illite; however a number of subsequent processes masking the primary fluid composition could be either proven or strongly implied. These processes include the dissolution of halite as well as anhydrite or gypsum, the precipitation of calcium carbonate and dolomite, and potentially the admixing of evaporated brines.

Very strong enrichments of the minor elements Li and B (CAMV and Bonjardim MV) suggest high temperature alterations (>150 °C) related to fluid mobilisation along fault systems cutting deeply into the underlying basement. Element enrichments may be caused by elevated concentrations in rising hydrothermal fluids and/or additional leaching of these elements from the sediments at higher temperatures. A compilation of various hot and cold vent sites (Fig. 10) suggests that strong Li enrichments in combination with moderate B/Li ratios may be a good indicator for this type of processes. At least at CAMV, this observation is in line with the composition of

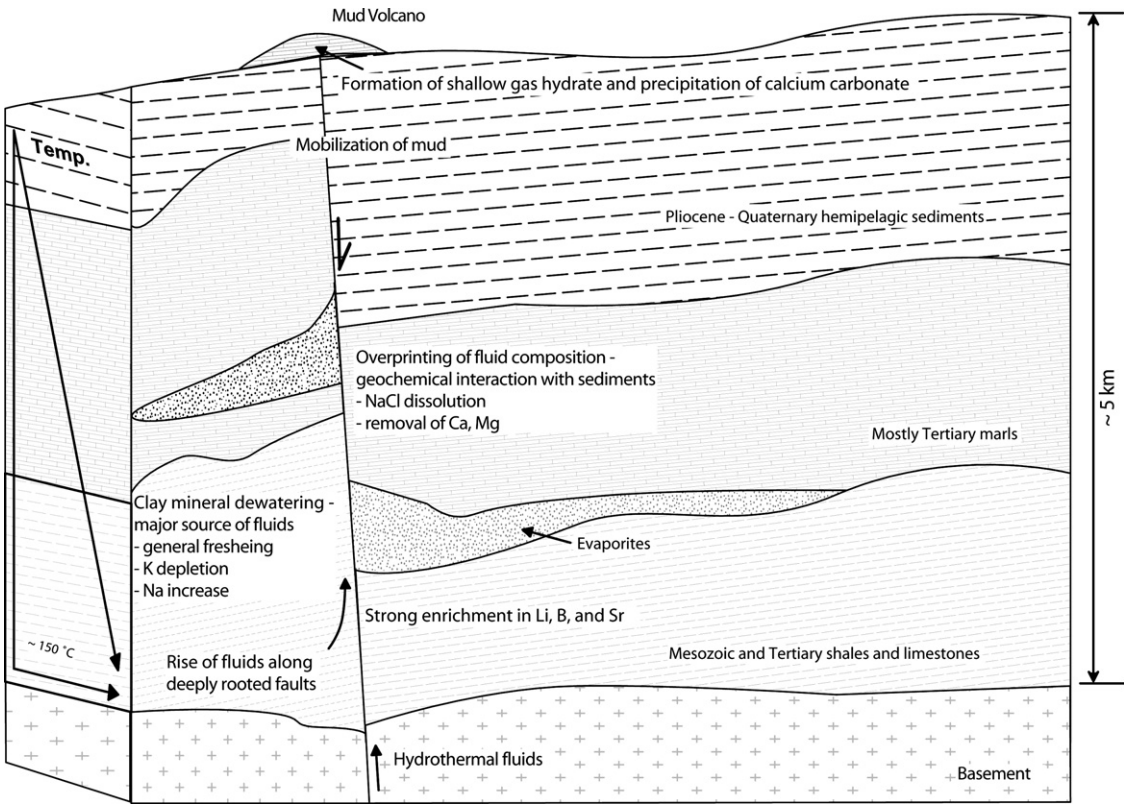

Fig. 11. Sketch illustrating an idealized sequence of MV fluid forming processes in the Gulf of Cadiz.

CH_4-enriched, light volatile hydrocarbon gases. In addition, correlations between Li, B, and Sr, particularly at Bonjardim MV and CAMV, suggest that elevated Sr concentrations result from long-term leaching of crustal rocks and sediments, whereas differences in $^{87}Sr/^{86}Sr$ ratios may be caused by differences in the nature of underlying crustal material (oceanic vs. continental).

All processes discussed in this study are summarized in a simplified diagram (Fig. 11) showing the suggested flow path of the fluids along major faults cutting through an idealized sequence of sedimentary rocks in the Gulf of Cadiz (after Medialdea et al., 2004). Although the occurrence of a number of processes cannot be resolved unambiguously, the suggested interpretation provides a comprehensive overview and raises the important question to what extent higher temperature reactions, perhaps in underlying basement, are linked to the processes controlling mud volcanism and seepage of cold vents in general. However, the overall driving force of mud volcanism in the Gulf of Cadiz is—as in many accretionary and non-accretionary margins—clearly caused by clay mineral transformation.

Acknowledgments

We thank the officers, crew, and shipboard scientific party of RV Sonne for support at sea during expedition SO-175. Thanks to Kristin Nass, Mathias Marquardt, and Nadja Neubert for assistance in pore water sampling and processing on board and Bettina Domeyer, Anke Bleyer, and Regina Surberg for analyses performed at IFM-GEOMAR. Marianne Nuzzo and Ed Hornibrook thank the DGM-INETI (Alfragide, Portugal) for use of laboratory space before and after the RV Sonne cruise. Klaus Wallmann is thanked for many fruitful discussions on this topic. The manuscript benefited significantly from comments by Giovanni Aloisi and two anonymous reviewers. This work was supported by the Sonderforschungsbereich 574 at Christian-Albrechts-Universität, Kiel (SFB publication N° 103), Fundação para a Ciência e a Tecnologia (Lisbon, Portugal), EU-METROL, and the Eurocores/Euromargins MVSEIS Project (01-LEC-EMA24F; PDCTM72003/DIV/40018).

Associate editor: Jeffrey C. Alt

References

Aloisi, G., Drews, M., Wallmann, K., Bohrmann, G., 2004a. Fluid expulsion from the Dvurechenskii mud volcano (Black Sea). Part I. Fluid sources and relevance to Li, B, Sr, I and dissolved inorganic nitrogen cycles. *Earth Planet. Sci. Lett.* **225**, 347–363.

Aloisi, G., Wallmann, K., Bollwerk, S.M., Derkachev, A., Bohrmann, G., Suess, E., 2004b. The effect of dissolved barium on biogeochemical processes at cold seeps. *Geochim. Cosmochim. Acta* **68** (8), 1735–1748.

Argus, D.F., Gordon, R.G., Demets, C., Stein, S., 1989. Closure of the Africa–Eurasia–North America plate motion circuit and tectonics of the Gloria fault. *J. Geophys. Res.* **94**, 5585–5602.

Banner, J.L., 2004. Radiogenic isotopes: systematics and applications to earth surface processes and chemical stratigraphy. *Earth-Sci. Rev.* **65**, 141–194.

Baptista, M.A., Heitor, S., Miranda, J.M., Miranda, P., Mendes Vitor, L., 1988. The 1755 Lisbon tsunami; evaluation of the tsunami parameters. *J. Geodyn.* **25** (2), 143–157.

Behrens, E.W., 1988. Geology of a continental slope oil seep, Northern Gulf of Mexico. *AAPG Bull.* **72** (2), 105–114.

Bernasconi, S.M. 1999. Interstitial water chemistry in the Western Mediterranean: results from leg 161. *Proceedings of the Ocean Drilling Program, Scientific Results* **161**, pp. 423–432.

Boles, J.R., Franks, S.G., 1979. Clay diagenesis in Wilcox sandstones of southwest Texas: implications of smectite diagenesis on sandstone cementation. *J. Sed. Petrol.* **49**, 55–70.

Boudreau, B.P., 1997. *Diagenetic models and their implementation: modelling transport and reactions in aquatic sediments*. Springer, Berlin, Heidelberg.

Bowes, H.L., Hornibrook, E.R.C., 2006. Emission of highly ^{13}C-depleted methane from an upland blanket mire. *Geophys. Res. Lett.* **33**, L04401. doi:10.1029/2005GL025209.

Brown, K.M., Saffer, D.M., Bekins, B.A., 2001. Smectite diagenesis, pore water freshening, and fluid flow at the toe of the Nankai wedge. *Earth Planet. Sci. Lett.* **194**, 97–109.

Brumsack, H.-J., Zuleger, E., 1992. Boron and boron isotopes in pore waters from ODP Leg 127, Sea of Japan. *Earth Planet Sci. Let.* **113**, 427–433.

Buffett, B., Archer, D., 2004. Global inventory of methane clathrate: sensitivity to changes in the deep ocean. *Earth Planet. Sci. Lett.* **227**, 185–199.

Buforn, E., Sanz de Galeano, C., Udias, A., 1995. Seismotectonics of Ibero-Maghrebian region. *Tectonophysics* **248**, 247–261.

Burke, W.H., Denison, R.E., Hetherington, E.A., Koepnik, R.B., Nelson, H.F., Otto, J.B., 1982. Variation of seawater ^{87}Sr/^{86}Sr throughout Phanerozoic time. *Geology* **10**, 516–519.

Chamley, H., 1989. *Clay sedimentology*. Springer-Verlag, Berlin.

Chamot-Rooke, N., Rabaute, A., Kreemer, C., 2005. Western Mediterranean Ridge mud belt correlates with active shear strain at the prism-backstop geological contact. *Geology* **33** (11), 861–864.

Chan, L.-H., Kastner, M., 2000. Lithium isotopic compositions of pore fluids and sediments in the Costa Rica subduction zone: implications for fluid processes and sediment contribution to the arc volcanoes. *Earth Planet Sci. Let.* **183**, 275–290.

Chan, L.H., Leeman, W.P., You, C.-F., 1999. Lithium isotopic composition of Central American volcanic arc lavas: implications for modification of subarc mantle by slab-derived fluids. *Chem. Geol.* **160**, 255–280.

Cuadros, J., 2006. Modeling of smectite illitization in burial diagenesis environments. *Geochim. Cosmochim. Acta* **70**, 4181–4195.

Dählmann, A., De Lange, G.J., 2003. Fluid-sediment interactions at Eastern Mediterranean mud volcanoes: a stable isotope study from ODP Leg 160. *Earth Planet. Sci. Lett.* **212**, 377–391.

De Lange, G.J., Brumsack, H.-J., 1998. Pore-water indications for the occurrence of gas hydrates in eastern mediterranean mud dome structures. *Proceedings of the Ocean Drilling Program, Scientific Results* **160**, pp. 569–574.

Depreiter, D., Poort, J., Van Rensbergen, P., Henriet, J.P., 2005. Geophysical evidence of gas hydrates in shallow submarine mud volcanoes on the Moroccan margin. *J. Geophys. Res.* **110**, B10103. doi:10.1029/2005JB003622.

Dia, A.N., Castrec, M., Boulègue, J., Boudou, J.P., 1995. Major and trace element and Sr isotope constraints on fluid circulations in the Barbados accretionary complex. Part I: Fluid origin. *Earth Planet. Sci. Lett.* **134**, 69–85.

Duarte, J.C., Rosas, F., Pinheiro, L.M., Matias, L.M., Carvalho, A.M., Terrinha, P., Ivanov, M., 2005. Interpretation of recent sedimentary and tectonic structures off SW Iberia from multibeam bathymetry, seismic reflection and experimental modelling. in: *Geophysical Research Abstracts*, vol. 7, 07867. European Geosciences Union 2005.

Freed, R.L., Peacor, D.R., 1989. Variability in temperature of the smectite/illite reaction in Gulf Coast sediments. *Clay Miner.* **24**, 171–180.

Fryer, P., Wheat, C.G., Mottl, M.J., 1999. Mariana blueschist mud volcanism: implications for conditions within the subduction zone. *Geology* **27** (2), 103–106.

Gardner, J.M., 2001. Mud volcanoes revealed and sampled on the western Morrocan continental margin. *Geophys. Res. Lett.* **28** (2), 339–342.

Godon, A., Jendrzejewski, N., Castrec-Rouelle, M., Dia, A., Pineau, F., Boulegue, J., Javoy, M., 2004. Origin and evolution of fluids from mud volcanoes in the Barbados accretionary complex. *Geochim. Cosmochim. Acta* **68** (9), 2153–2165.

Gonzalez-Fernandez, A., Cordoba, D., Matias, L., Torne, M., 2001. Seismic crustal structure in the Gulf of Cadiz (SW Iberian Peninsula). *Mar. Geophys. Res.* **22**, 207–223.

Gràcia, E., Danobeitia, J., Verges, J., PARCIFAL-TEAM, 2003. Mapping active faults offshore Portugal (36°N–38°N): implications for seismic hazard assessment along the southwest Iberian margin. *Geology* **31**(1), pp. 83–86.

Grasshoff, K., Ehrhardt, M., Kremling, K., 1983. *Methods of Seawater Analysis*. Verlag Chemie, Weinheim.

Gutscher, M.-A., 2004. What caused the Great Lisbon earthquake? *Science* **305**, 1247–1248.

Gutscher, M.-A., Malod, J., Rehault, J.-P., Contrucci, I., Klingelhoefer, K., Mendes-Victor, L., Spakman, W., 2002. Evidence for active subduction beneath Gibraltar. *Geology* **30** (12), 1071–1074.

Haese, R., Hensen, C., De Lange, G.J., 2006. Pore water geochemistry of eastern Mediterranean mud volcanoes: implications for fluid transport and fluid origin. *Mar. Geol.* **225**, 191–208.

Haese, R.R., Meile, C., Van Cappellen, P., De Lange, G.J., 2003. Carbon geochemistry of cold seeps: methane fluxes and transformation in sediments from Kazan mud volcano, eastern Mediterranean Sea. *Earth Planet. Sci. Lett.* **212**, 361–375.

Henry, P., Le Pichon, X., Lallemant, S., Lance, S., Martin, J.B., Foucher, J.-P., Fiala-Médioni, A., Rostek, F., Guilhaumou, N., Pranal, V., Castrec, M., 1996. Fluid flow in and around a mud volcano field seaward of the Barbados accretionary wedge: results from Manon cruise. *J. Geophys. Res.* **101** (B9), 20297–20323.

Hensen, C., Wallmann, K., 2005. Methane formation at Costa Rica continental margin—constraints for gas hydrate inventories and cross-décollement fluid flow. *Earth Planet. Sci. Lett.* **236**, 41–60.

Hensen, C., Wallmann, K., Schmidt, M., Ranero, C.R., Suess, E., 2004. Fluid expulsion related to mud extrusion off Costa Rica continental margin—a window to the subducting slab. *Geology* **32**, 201–204.

Ivanenkov, V.N., Lyakhin, Y.I., 1978. Determination of total alkalinity in seawater. In: Bordovsky, O.K., Ivanenkov, V.N. (Eds.), *Methods of Hydrochemical Investigations in the Ocean (in Russian)*. Nauka Publ. House, Moscow, pp. 110–114.

Kopf, A., Deyhle, A., Lavrushin, V.Y., Polyak, B.G., Gieskes, J.M., Buachidze, G.I., Wallmann, K., Eisenhauer, A., 2003. Isotopic evidence (He,B,C) for deep fluid and mud mobilization from mud volcanoes in the Caucasus continental collission zone. *Int. J. Earth Sci.* **92**, 407–425.

Kopf A. and Participants a. c., 2004. Report and preliminary results of Sonne cruise SO-175, Miami-Bremerhaven, 12.11.-30.12.2003. Berichte, Fachbereich Geowissenschaften, Universität Bremen, No. 228.

Lonergan, L., White, N., 1997. Origin of the Betic–Rif mountain belt. *Tectonics* **16** (3), 504–522.

Luff, R., Wallmann, K., 2003. Fluid flow, methane fluxes, carbonate precipitation and biogeochemical turnover in gas hydrate-bearing sediments at Hydrate Ridge, Cascadia Margin: numerical modeling and mass balances. *Geochim. Cosmochim. Acta* **67** (18), 3403–3421.

Maestro, A., Somoza, L., Medialdea, T., Talbot, C.J., Lowrie, A., Vazquez, J.T., Diaz-del-Rio, V., 2003. Large-scale slope failure involving Triassic and Middle Miocene salt and shale in the Gulf of Cadiz (Atlantic Iberian Margin). *Terra Nova* **15**, 380–391.

Maldonado, A., Somoza, L., Pallares, L., 1999. The Betic orogen and the Iberian–African boundary in the Gulf of cadiz: geological evolution (central North Atlantic). *Mar. Geol.* **155**, 9–43.

Martin, J.B., Gieskes, J.M., Torres, M.E., Kastner, M., 1993. Bromine and iodine in Peru margin sediments and pore fluids: implications for fluid origins. *Geochim. Cosmochim. Acta* **57**, 4377–4389.

Martin, J.B., Kastner, M., Elderfield, H., 1991. Lithium: sources in pore fluids of Peru slope sediments and implications for oceanic fluxes. *Mar. Geol.* **102**, 281–292.

Martin, J.B., Kastner, M., Henry, P., Le Pichon, X., Lallement, S., 1996. Chemical and isotopic evidence for sources of fluids in a mud volcano field seaward of the Barbados accretionary wedge. *J. Geophys. Res.* **101** (B9), 20325–20345.

Mazurenko, L.L., Soloviev, V.A., Gardner, J.M., Ivanov, M.K., 2003. Gas hydrates in the Ginsburg and Yuma mud volcano sediments (Moroccan margin): results of chemical and isotopic studies of pore water. *Mar. Geol.* **195**, 201–210.

McCaffrey, M.A., Lazar, B., Holland, H.D., 1987. The evaporation of seawater and the coprecipitation of Br^- and K^+ with halite. *J. Sediment. Petrol.* **57**, 928–937.

Medialdea, T., Vegas, R., Somoza, L., Vazquez, J.T., Maldonaldo, A., Diaz-del-Rio, V., Maestro, A., Cordoba, D., Fernandez-Puga, M.C., 2004. Structure and evolution of the 'olistostrome' complex of the Gibraltar Arc in the Gulf of cadiz (eastern Central Atlantic): evidence from two long seismic cross-sections. *Mar. Geol.* **209**, 173–198.

Meghraoui, M., Morel, J.-L., Andrieux, J., Dahmani, M., 1996. Tectonique plio-quaternaire de la chaine tello-rifaine et de la mer d'Alboran. Une zone complexe de la convergence continent–continent. *Bull. Soc. Geol. France* **167** (1), 141–157.

Milkov, A.V., 2000. Worldwide distribution of submarine mud volcanoes and associated gas hydrates. *Mar. Geol.* **167**, 29–42.

Milkov, A.V., Sassen, R., Apanasovich, T.V., Dadashev, F.G., 2003. Global gas flux from mud volcanoes: a significant source of fossil methane in the atmosphere and the ocean. *Geophys. Res. Lett.* **30** (2), 1037. doi:10.1029/2002GL016358.

Moore, J.C., Mascle, A., 1987. Expulsion of fluids from depth along a subdution zone decollement horizon. *Nature* **326**, 785–788.

Moore, J.C., Vrolijk, P., 1992. Fluids in accretionary prisms. *Rev. Geophys.* **30** (2), 113–135.

Morel, J.-L., Meghraoui, M., 1996. Goringe-Alboran-Tell tectonic zone: a transpression system along the Africa–Eurasia plate boundary. *Geology* **24** (8), 755–758.

Morse, J.W., Mackenzie, F.T., 1990. *Geochemistry of Sedimentary Carbonates*. Elsevier, Amsterdam.

Niemann, H., Duarte, J., Hensen, C., Omoregie, E., Magalhães, V.H., Elvert, M., Pinheiro, L.M., Boetius, A., Kopf, A., 2006. Microbial methane turnover at mud volcanoes of the Gulf of Cadiz. *Geochim. Cosmochim. Acta* **70**, 5336–5355.

Niewöhner, C., Hensen, C., Kasten, S., Zabel, M., Schulz, H.D., 1998. Deep sulfate reduction completely mediated by anaerobic methane oxidation in sediments of the upwelling area off Namibia. *Geochim. Cosmochim. Acta* **62** (3), 455–464.

L.M. Pinheiro, Ivanov, M., Kenyon, N., Magalhães, V.H., Somoza, L., Gardner, J.M., Kopf, A., Van Rensbergen, P., Monteiro, J.H., Euromargins-MVSEIS-Team., 2005. Structural control of mud volcanism and hydrocarbon-rich fluid seepage in the Gulf of Cadiz: results from the TTR-15 and other previous cruises. *CIESM Workshop Monograph*, 28.

Pinheiro, L.M., Ivanov, M.K., Sautkin, A., Akhmanov, G., Magalhaes, V.H., Volkonskaya, A., Monteiro, J.H., Somoza, L., Gardner, J.V., Hamouni, N., Cunha, M.R., 2003. Mud volcanism in the Gulf of Cadiz: results from the TTR-10 cruise. *Mar. Geol.* **195**, 131–151.

Reicherter, K.R., Pletsch, T.K., 2000. Evidence for a synchronous circum-Iberian subsidence event and its relation to the African–Iberian plate convergence in the Late Cretaceous. *Terra Nova* **12** (3). doi:10.1046/j.1365-3121.2000.123276.x.

Ribeiro, A., Cabral, J., Baptista, R., Matias, L., 1996. Stress pattern in Portugal mainland and the adjacent Atlantic region, West Iberia. *Tectonics* **15** (2), 641–659.

Saffer, D.M., Bekins, B.A., 1999. Fluid budgets at convergent plate margins: implications for the extent and duration of fault zone dilation. *Geology* **27**, 1095–1098.

Sartori, R., Torelli, l., Zitellini, N., Peis, D., Lodolo, E., 1994. Eastern segment of the Azores-Gibraltar line (Central-Eastern Atlantic): an oceanic plate boundary with diffuse compressional deformation. *Geology* **22**, 555–558.

Schmidt, M., Hensen, C., Mörz, T., Müller, C., Grevemeyer, I., Wallmann, K., Mau, S., Kaul, N., 2005. Methane hydrate accumulation in "Mound 11" mud volcano, Costa Rica forearc. *Mar. Geol.* **216**, 83–100.

Sheppard, S.M.F., Gilg, H.A., 1996. Stable isotope geochemistry of clay minerals. *Clay Miner.* **31**, 1–24.

Spinelli, G.A., Underwood, M.B., 2004. Character of sediments entering the Costa Rica subduction zone: Implications for partitioning of water along the plate interface. *The Island Arc* **13**, 432–451.

Stadnitskaia, A., Ivanov, M.K., Blinova, V., Kreulen, R., van Weering, T.C.E., 2006. Molecular and carbon isotopic variability of hydrocarbon gases from mud volcanoes in the Gulf of Cadiz, NE Atlantic. *Mar. Petrol. Geol.* **23** (3), 281–296.

Suess, E., Bohrmann, G., Von Huene, R., Linke, P., Wallmann, K., Lammers, S., Sahling, H., Winckler, G., Lutz, R.A., Orange, D., 1998. Fluid venting in the eastern Aleutian subduction zone. *J. Geophys. Res.* **103** (B2), 2597–2614.

Thornton, E.C., Seyfried Jr., W.E., 1987. Reactivity of organic-rich sediment in seawater at 350 °C, 500 bars: experimental and theoretical constraints and implications for the Guaymas Basin hydrothermal system. *Geochim. Cosmochim. Acta* **51**, 1997–2010.

Tishchenko, P., Hensen, C., Wallmann, K., Wong, C.S., 2005. Calculation of the stability and solubility of methane hydrate in seawater. *Chem. Geol.* **219**, 37–52.

Tobin, H.J., Moore, J.C., Mackay, M.E., Orange, D.L., Kulm, L.D., 1993. Fluid flow along a strike–slip fault at the toe of the Oregon accretionary prism: implications for the geometry of frontal accretion. *Geol. Soc. Am. Bull.* **105** (5), 569–582.

Van Rensbergen, P., Depreiter, D., Pannemans, B., Moerkerke, G., Van Rooij, D., Marsset, B., Akhmanov, G., Blinova, V., Ivanov, M., Rachidi, M., Magalhães, V., Pinheiro, L.M., Cunha, M., Henriet, J.-P., 2005. The El Arraiche mud volcano field at the Moroccan Atlantic slope, Gulf of Cadiz:. *Mar. Geol.* **219**, 1–369.

Von Damm, K.L., 1990. Seafloor hydrothermal activity: black smoker chemistry and chimneys. *Ann. Rev. Earth Planet. Sci.* **18**, 173–204.

Von Damm, K.L., Edmond, J.M., Measures, C.I., Grant, B., 1985. Chemistry of submarine hydrothermal solutions at Guaymas Basin, Gulf of California. *Geochim. Cosmochim. Acta* **49** (11), 2221–2237.

Von Damm, K.L., Parker, C.M., Zierenberg, R.A., Lilley, M.D., Olson, E.J., Clague, D.A., McClain, J.S., 2005. The Escanaba Trough, Gorda Ridge hydrothermal system: Temporal stability and subseafloor complexity. *Geochim. Cosmochim. Acta* **69** (21), 4971–4984.

Wallace, P.J., Dickens, G.R., Paull, C.K., Ussler III, W., 2000. Effects of core-retrieval and degassing on the carbon isotope composition of methane in gas hydrate and free gas-bearing sediments from the Blake Ridge. In: Paull, C.K., Matsumoto, R., Wallace, P.J., Dillon, W.P. (Eds.), *Proc. ODP, Sci. Res.*, vol. 164, pp. 101–112.

You, C.-F., Gieskes, J.M., 2001. Hydrothermal alteration of hemi-pelagic sediments: experimental evaluation of geochemical processes in shallow subduction zones. *Appl. Geochem.* **16**, 1055–1066.

You, C.-F., Spivack, A.J., Gieskes, J.M., Rosenbauer, R., Bischoff, J.L., 1995. Experimental study of boron geochemistry: implications for fluid processes in subduction zones. *Geochim. Cosmochim. Acta* **59** (12), 2435–2442.

You, C.-F., Spivack, A.J., Smith, J.H., Gieskes, J.M., 1993. Mobilization of boron in convergent margins: implications for the boron geochemical cycle. *Geology* **21**, 207–210.

Zeyen, H., Ayarza, P., Fernandez, M., Rimi, A., 2005. Lithospheric structure under the western African–European plate boundary: a transect across the Atlas Mountains and the Gulf of Cadiz. *Tectonics* **24** (2). doi:10.1029/2004TC001639.